

Constructing A 3D Finite Element Model To Investigate the Structural Behavior of LCP, DCP & LC-DCP Used In the Fixation of Long Bones

Gaffar Gailani
Mechanical Engineering Department
Graduate Center of CUNY
ggailani@gc.cuny.edu

Sidi Berri
Department of Mechanical Engineering Tech.
New York City College of Technology
sberri@citytech.cuny.edu

Ali Sadegh
Mechanical Engineering Department
City College of New York
Sadegh@ccny.cuny.edu

Abstract

Limited investigations have been performed in the area of generating three dimensional (3D) finite element (FE) models that can predict the structural behavior of bone and implant interface in the internal fixation of long bones. Current experimental techniques do not provide the data needed for evaluating these complex areas [3]. Imported models from Computer Aided Design (CAD) packages cannot address the non-linearity issues associated with contact, as well as the complex geometry. In addition, to the reduced accuracy different designs of plates and screws were introduced based primarily on experimental results. In this paper, a new approach to constructing this model is proposed. The new approach requires discretizing the geometry and the finite element mesh. Results are obtained for different types of loads, including cyclic external loads and static tensile preloads. The model can accommodate Dynamic Compression Plates (DCP); Locked Compression Plates (LCP); and Low Contact Dynamic Compression Plates (LC-DCP), as well as the design of new plates. A meshing technique based on the nodes shared in the boundaries was adopted to mesh the large number of surfaces produced by 180 volumes. Rigid Links were created to represent the locking feature of LCP. The FE model has shown many advantages, such as flexibility in geometry and quantifying results that were predicted theoretically. The model is easily modified to fit many geometrical or other design changes without remeshing. This will aid in optimizing the design of the plates used in the internal fixation of long bones. The model can analyze the micro-motion among the plate, screws and the bone. The magnitude of this motion is believed to have influence on the formation of the fibrous tissue around the implants, which is assumed to be one of the causes of the loosening of implants [5].

Introduction

Internal fixation of long bones using plates has been practiced for more than 100 years. The method has become increasingly popular since World War II. In the early stages of fracture repair the function of an internal fixation procedure was to immobilize the fracture fragments. This allowed bony union to proceed [4]. The internal fixation of fractures, Fig.(1), has evolved in recent decades with a change of emphasis from mechanical to biological priorities. Recently, internal fixation underwent a basic evolution. The new objective is to achieve maximum stabilization with minimum damage to the blood supply during fracture repair. Biological internal fixation needs to be improved based on today's understanding of biology, biomechanics and mechanics in order to provide better and safer fracture treatment.

The concept of biological internal fixation is still developing. There is controversy surrounding the rigidity of the plates that are currently in use. In addition, there are incidents of bone refracture, screw and fatigue failures. There is a need for research, as well as the development of structural analysis tools to evaluate current and future internal fixation plate designs. The goal is to produce a plate that has the required strength to promote fracture healing, and not very stiff so as to hinder bone remodeling. The contradiction exists because there is a need for extremely rigid fixation during the healing of fractures, and less rigid fixation during later bone remodeling. This remains an enigma in orthopedic surgery.

Numerous models have been used to study the internal fixation of long bones. Simon and Woo [3] used very simplified 1D, 2D & 3D models, concluding that these models needed improvement to quantify the stresses and strains in critical areas. Ganesh and Ramarkrishna [10] utilized a 2D FE model to introduce a new design of plates based on graded stiffness. Numerous 2D FE models have been developed for the analysis of plated and non-plated long bones. Inherent in all these studies were unknown errors associated with a 2D approximation of a complex 3D problem. Cordey and Perren [5] proposed the composite beam theory approach to analyze the bone and the plate as a composite beam. The composite beam theory has its own limitations, such as deficiency in analyzing the micro-motion between the plate and the bone.

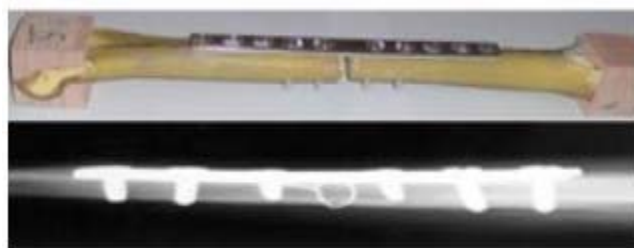


Fig (1): Experimental and real life models of bone fracture repair

Many new plate designs were introduced recently such as: Locked Plates (see fig. 2); Point Contact Fixators (PC-Fix); Stiffness Graded; and Biodegradable. Most of these

designs, if not all, were not associated with FE analysis in 3D. The 3D analysis was important to quantify the improvement with respect to the conventional plates, as well as sketching guidelines for the direction of the development of new designs.

Methods

The complexity of the geometry is a fact that the FE model needs to consider. The geometry of the whole assembly has been discretized numerous times (as shown in fig. 3), in order to reduce computational costs, and to create a flexible geometrical model that can be modified to match the design of different implants. The discretization will create more structural mesh that is well distributed over the model, and help in the meshing algorithm where contact surfaces need to be selected. Automatic Dynamic Incremental Nonlinear Analysis software (ADINA) was used for the FE analysis.

Figs.(3) and (4). The prism volumes were used to fit the conical shape of the screw head, as well as the whole screw shaft. Four cylindrical coordinate systems and one cartesian coordinate system were used to create the DGM.

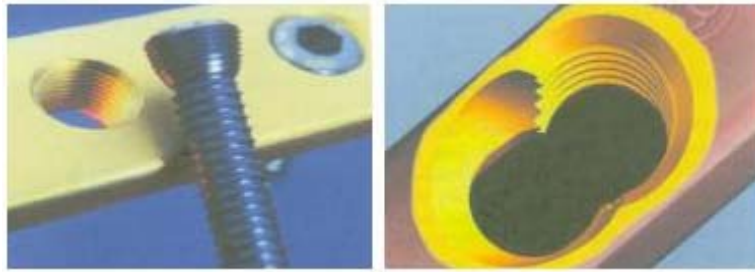


Fig (2): Different designs of LCP

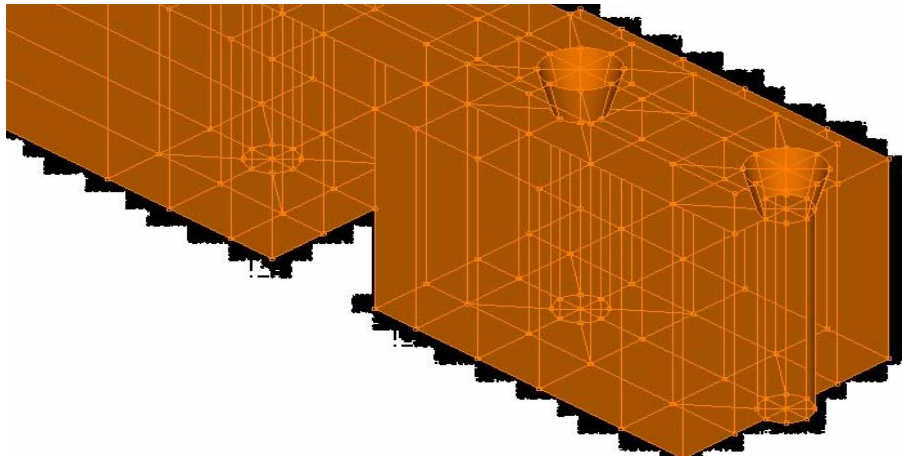


Fig (3): Constructing the DGM

The material properties for the plate and screws are the same. Steel or titanium is used to make the plate and screws. It should be noted that there are many published papers on

the study of the mechanical properties of bones. The bone is treated as an orthotropic material due to the variation of the module of elasticity (E) in the longitudinal, and the transversal directions of the bone. It is important to mention that bone is slightly viscoelastic, and its measured Young’s modulus is to some extent strain rate dependent [13].

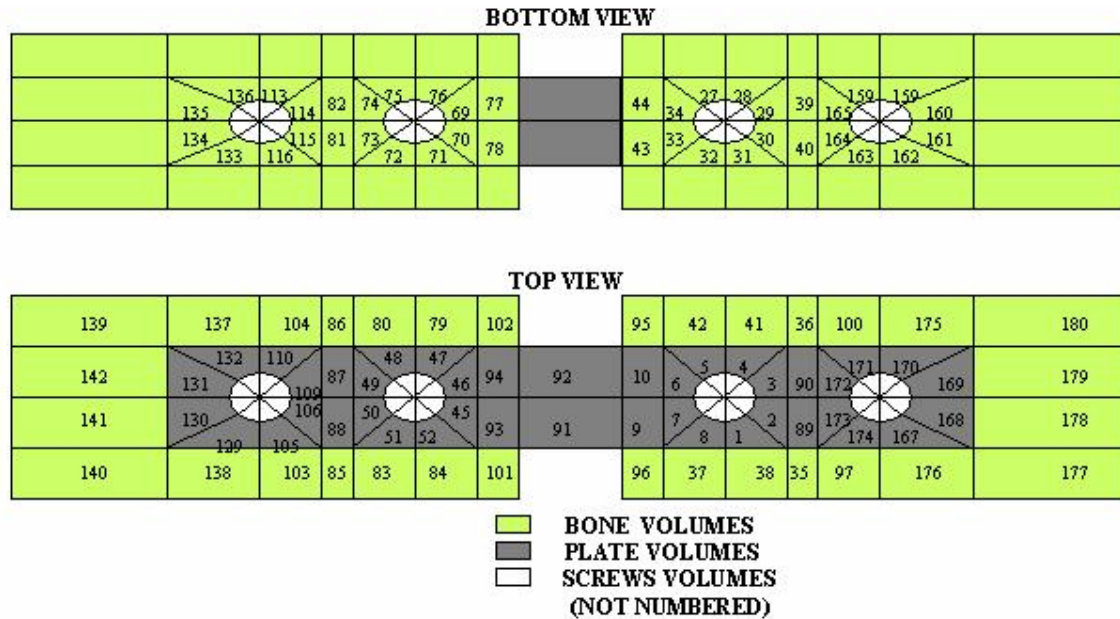


Fig (4): Top and bottom views of the DGM

The meshing process was done, so that it could accommodate the numerous contact surfaces, as well as the continuity of the model components. A specific meshing technique based on Nodal Coincidence Checking was applied to mesh the model. The algorithm or the technique was easily explained for limited number of contact surfaces in 2D. It should be capable of dropping 2 nodes at the same point along the contact edges, and only one node where there is no contact. Figure (5) illustrates this concept. The same procedure could be followed in 3D with some complexity.

The meshing technique should assign any number of nodes at the participating edges and vertices along L2 or L4. However, it should not assign any extra nodes at the edges that are part of the continuum. In order to understand this technique it is important to visualize an imaginary surface S3, and it is adjacent to S2, or S1. Therefore, the nodes only will be shared at the edges of S3 and S2, or S1.

In Fig (6) a brief idea of how the contact surfaces will be meshed in 3D is introduced. The surface of V1, S1, is in contact with the surface of V2, S1. S4 in V1, and S2 in V3 are identical because both of them belong to the screw. Therefore, it is expected that the meshing algorithm should have the two separate surfaces of the screw, S1 and S2, sharing the same nodes. The contact between the plate and the bone is demonstrated by the contact of S4 in V2 and S2 in V4. The meshing algorithm should allow no sharing of nodes between these two surfaces. There will be two nodes at every point to allow

contact in the initial configuration. The same procedure will be applied for the contact between the screw and the bone. As a check, after the completion of the mesh two nodes should be detected at the boundary of V1 and V2. Notice that P1 and P2 of V1 have the same coordinates of P2 and P1 of V2. Three nodes should be detected at P1 and P2 of V3 because these coordinates are shared among the former, P3 and P4 of V2, and P1 and P2 of V4. If the contact between the screw and the bone is ignored then the number of nodes in the boundary will drop from 3 to 2 nodes. The key point is that both S1 in V1 and V2 have exactly the same coordinates, which demonstrate the initial configuration - the screw head is in full contact with the plate hole. The distribution technique of the nodes is demonstrated in Table (1).

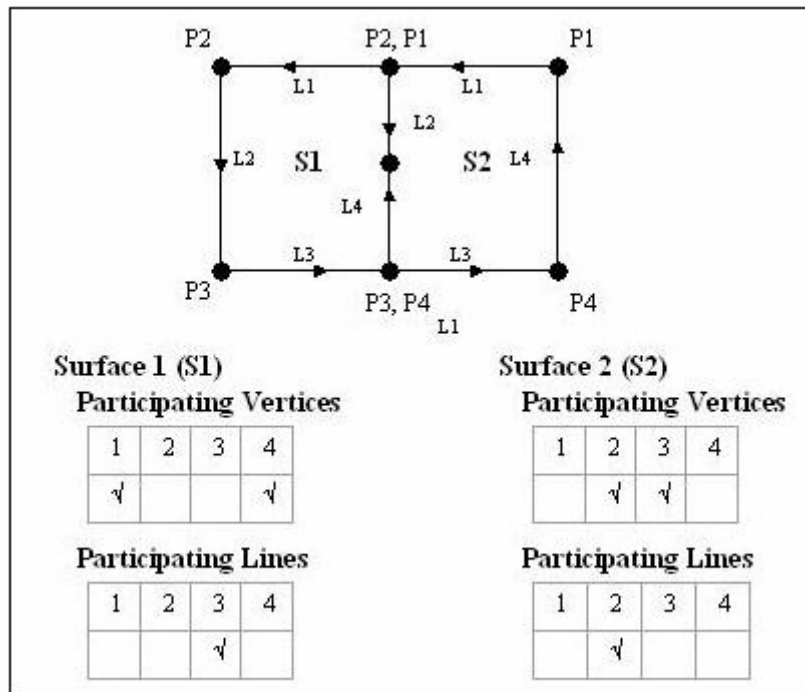


Fig (5): meshing of contact edges in 2D

The mesh order is a very important element in the meshing process. In Table (1) it is clear that the mesh process for V1 is different from V3. The meshing of V3 ignored vertices 1 and 2 due to the fact that two nodes were already assigned there from the meshing of V1. The assumption is that V1 was meshed before V3. In addition, it must be noted that V1 and V4 belonged to the same entity - the screw. The mesh would not be done on every individual volume, but rather take a set of volumes that exhibits certain geometrical symmetry and mesh the set by the same technique.

The mesh should be checked manually to guarantee that the algorithm has distributed the nodes according to the implemented procedure. This could be accomplished by selecting some arbitrary nodes in the boundaries. Once the mesh is created, the density of the mesh could be changed at any time, but it is always advisable to run the solution in the beginning for a low-density mesh, and increase the mesh density later. The assembly

mesh has used 3D 8-noded solid elements. The number of elements used is 4,608 elements for the bone, and 6,784 elements for the screws and the plate. The total number of nodes in the whole model is 13,488 nodes.

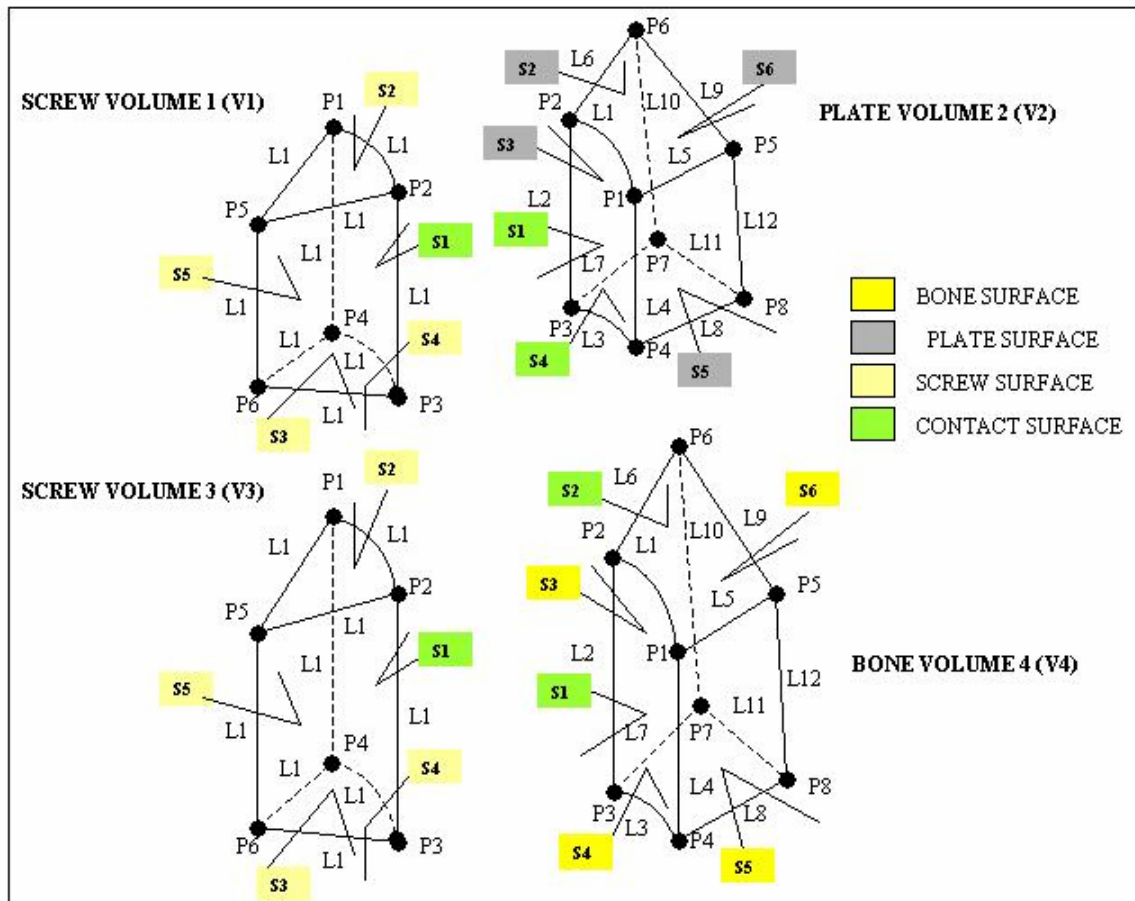


Fig (6): The meshing process with surfaces shown with their normals

The typical input line to mesh V2, assuming that V2 would be meshed last, should look like:

```

GVOLUM
NODES 8
NCFACE 2356
NCEDGE 569AC
NCVERTEX 56
GROUP 1
MESHING MAPPED
MIDNODES CURVED
VOL 2

```

The results are shown in Fig (7). At the last circular line that represents the boundary between the plate volume and the screw volume, the mesh algorithm has assigned two nodes at one point. There is a duplication of nodes. Furthermore, each node is

represented by a green number at each point, and can be clearly seen by selecting the node's number where the number appears to be overwritten.

Table (1): The nodes distribution technique.

VOLUME 1																																																						
Participating Vertices	Participating Lines	Participating Surfaces																																																				
<table border="1"> <tr><td>1</td><td>2</td><td>3</td><td>4</td><td>5</td><td>6</td></tr> <tr><td>√</td><td>√</td><td>√</td><td>√</td><td></td><td></td></tr> </table>	1	2	3	4	5	6	√	√	√	√			<table border="1"> <tr><td>1</td><td>2</td><td>3</td><td>4</td><td>5</td><td>6</td><td>7</td><td>8</td><td>9</td></tr> <tr><td>√</td><td>√</td><td>√</td><td>√</td><td></td><td></td><td></td><td></td><td></td></tr> </table>	1	2	3	4	5	6	7	8	9	√	√	√	√						<table border="1"> <tr><td>1</td><td>2</td><td>3</td><td>4</td><td>5</td></tr> <tr><td>√</td><td></td><td></td><td></td><td></td></tr> </table>	1	2	3	4	5	√																
1	2	3	4	5	6																																																	
√	√	√	√																																																			
1	2	3	4	5	6	7	8	9																																														
√	√	√	√																																																			
1	2	3	4	5																																																		
√																																																						
VOLUME 2																																																						
Participating Vertices	Participating Lines	Participating Surfaces																																																				
<table border="1"> <tr><td>1</td><td>2</td><td>3</td><td>4</td><td>5</td><td>6</td><td>7</td><td>8</td></tr> <tr><td>√</td><td>√</td><td>√</td><td>√</td><td></td><td></td><td>√</td><td>√</td></tr> </table>	1	2	3	4	5	6	7	8	√	√	√	√			√	√	<table border="1"> <tr><td>1</td><td>2</td><td>3</td><td>4</td><td>5</td><td>6</td></tr> <tr><td>√</td><td>√</td><td>√</td><td>√</td><td></td><td></td></tr> <tr><td>7</td><td>8</td><td>9</td><td>10</td><td>11</td><td>12</td></tr> <tr><td>√</td><td>√</td><td></td><td></td><td>√</td><td></td></tr> </table>	1	2	3	4	5	6	√	√	√	√			7	8	9	10	11	12	√	√			√		<table border="1"> <tr><td>1</td><td>2</td><td>3</td><td>4</td><td>5</td><td>6</td></tr> <tr><td>√</td><td></td><td></td><td>√</td><td></td><td></td></tr> </table>	1	2	3	4	5	6	√			√		
1	2	3	4	5	6	7	8																																															
√	√	√	√			√	√																																															
1	2	3	4	5	6																																																	
√	√	√	√																																																			
7	8	9	10	11	12																																																	
√	√			√																																																		
1	2	3	4	5	6																																																	
√			√																																																			
VOLUME 3																																																						
Participating Vertices	Participating Lines	Participating Surfaces																																																				
<table border="1"> <tr><td>1</td><td>2</td><td>3</td><td>4</td><td>5</td><td>6</td></tr> <tr><td></td><td></td><td>√</td><td>√</td><td></td><td></td></tr> </table>	1	2	3	4	5	6			√	√			<table border="1"> <tr><td>1</td><td>2</td><td>3</td><td>4</td><td>5</td><td>6</td><td>7</td><td>8</td><td>9</td></tr> <tr><td></td><td>√</td><td>√</td><td>√</td><td></td><td></td><td></td><td></td><td></td></tr> </table>	1	2	3	4	5	6	7	8	9		√	√	√						<table border="1"> <tr><td>1</td><td>2</td><td>3</td><td>4</td><td>5</td></tr> <tr><td>√</td><td></td><td></td><td></td><td></td></tr> </table>	1	2	3	4	5	√																
1	2	3	4	5	6																																																	
		√	√																																																			
1	2	3	4	5	6	7	8	9																																														
	√	√	√																																																			
1	2	3	4	5																																																		
√																																																						
VOLUME 4																																																						
Participating Vertices	Participating Lines	Participating Surfaces																																																				
<table border="1"> <tr><td>1</td><td>2</td><td>3</td><td>4</td><td>5</td><td>6</td><td>7</td><td>8</td></tr> <tr><td>√</td><td>√</td><td>√</td><td>√</td><td>√</td><td>√</td><td></td><td></td></tr> </table>	1	2	3	4	5	6	7	8	√	√	√	√	√	√			<table border="1"> <tr><td>1</td><td>2</td><td>3</td><td>4</td><td>5</td><td>6</td></tr> <tr><td>√</td><td>√</td><td>√</td><td>√</td><td>√</td><td>√</td></tr> <tr><td>7</td><td>8</td><td>9</td><td>10</td><td>11</td><td>12</td></tr> <tr><td></td><td></td><td>√</td><td></td><td></td><td></td></tr> </table>	1	2	3	4	5	6	√	√	√	√	√	√	7	8	9	10	11	12			√				<table border="1"> <tr><td>1</td><td>2</td><td>3</td><td>4</td><td>5</td><td>6</td></tr> <tr><td>√</td><td>√</td><td></td><td></td><td></td><td></td></tr> </table>	1	2	3	4	5	6	√	√				
1	2	3	4	5	6	7	8																																															
√	√	√	√	√	√																																																	
1	2	3	4	5	6																																																	
√	√	√	√	√	√																																																	
7	8	9	10	11	12																																																	
		√																																																				
1	2	3	4	5	6																																																	
√	√																																																					



Fig (7): Verification of the final mesh for the interface of plate volumes and screw volumes. The white arrow is pointing towards the boundary of V1 and V2

In order to accommodate the locking feature of the LCP as shown in Fig (1), Rigid Links need to be created. Rigid Links are special constraint equations established between two nodes- a master node and a slave node. As the nodes displace due to deformation, the slave node is constrained to translate and rotate, such that the distance between the master node and the slave node remains constant, and that the rotations at the slave node are the same as the corresponding rotations at the master node [11].

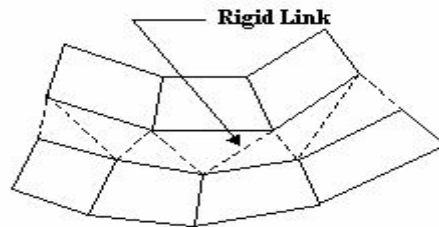


Fig (8): Mechanism of the Rigid Links.

The master and slave nodes should be decided based on the force transmitted from the bone to the implants, or vice versa. Likewise, the DCP should be modeled by choosing the contactor and target surfaces. Contact problems are nonlinear and there is no analytical solution for complex contact. The FE method is frequently used to determine the contact stresses and deformations.

Static and cyclic loads were used in the analysis. The static loads were in the pre-loading stage. The cyclic loads, for example bending moments and torsions, were considered to be external loads.

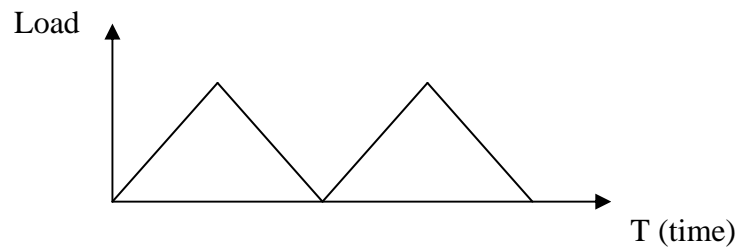


Fig (9): The cyclic external loads

Results

Results were obtained for different types of loading conditions, such as twisting and bending. Figure (10) shows the stress distribution in the LCP. Figure (11) shows the shear stress distribution in DCP (left), and the graph (right) shows the effective stresses on the top surface of the bone that is in contact with the plate¹.

¹ Simulations of this FE model can be viewed at www.adina.com/newsgrp, June 2006.

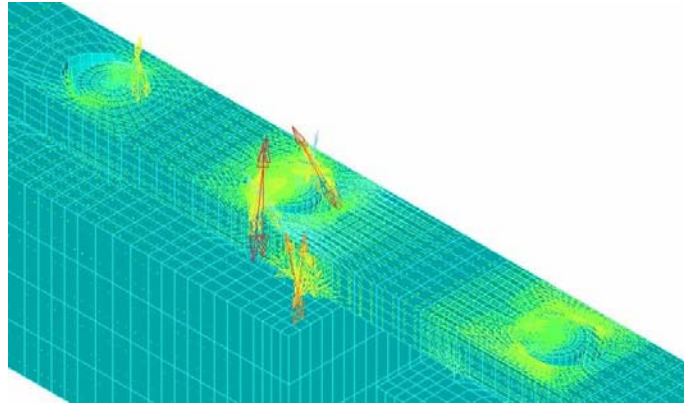


Fig (10): Stress vector in LCP subjected to bending.

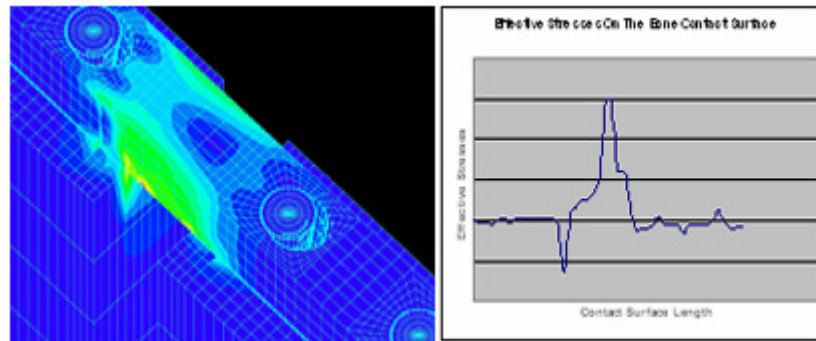


Fig (11): Shear stress distribution in DCP subjected to lateral bending (Left). The effective stress distribution on the bone contact surface for DCP (Right)

Discussion

LCP and DCP rely on different mechanical principles to provide fracture fixation. The results indicated that this model could be used to study the biological effects on the bone fracture fixation induced by using plates and screws, such as bone remodeling and formation of fibrous tissue around the implants. Bone remodeling is very sensitive to small changes in cyclic bone stresses that are produced by external cyclic loads.

In the late stages of fracture repair a loss of bone mass may occur. Many researchers attributed this loss to “Stress Shielding” which occurs as a result of structural adaptation of bone to reduced stress with the subsequent danger of refracture. One of the assumptions made is that the bone loss is a result of “plate induced osteopenia.” Cheal et al. concluded that disuse osteopenia should be limited to the central region between inner screws [8]. A result that is obviously seen in the FE model is high stresses were detected in the middle of the plate. High stresses between the plate and the bone may affect the cells in the periosteum layer as shown in Fig (12)

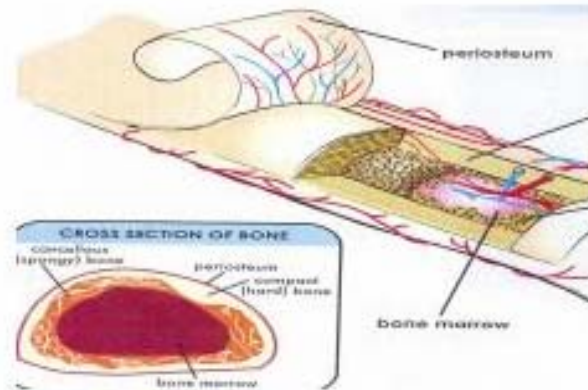


Fig (12): The effects of the plates on the bone structure

The stability of the implants is a major concern. One of the factors that affect this stability is the formation of fibrous tissue in the interface between the bone and the implants. This fibrous tissue loosens the implants, and leads to implant failure. There is some uncertainty as to the reason for this growth of fibrous tissue, but shear stress between the screw and the bone is suspected to be the cause of this formation [16]. This shear stress may originate from the bone-implant micro-motions. The in vivo study of Jasty et al. [17] showed that small amplitudes of micro-motion ($\leq 20 \mu\text{m}$) have no influence on the bone healing, but amplitudes greater than $150 \mu\text{m}$ produce a fibrous interface at a depth of 1 or 2 mm around the implants during the 6 weeks following the implantation. The FE model can predict the relationship between the micro-motion and the mechanical stimulus. This will be a subject for future communication.

The major advantage of the model is that it accommodates different geometries with minimum changes in the model. For example, Fig (2) shows two types of holes for LCP. One hole fits the screw's conical head exactly, and the other hole is bigger than the head of the screw. The latter provides a surgeon with the opportunity to change the location of the screw if necessary. The DGM can easily create the two different types of holes by moving 3 geometrical points backward and forward. Once these points are moved there should be no need for remeshing or reassigning of boundary conditions, and the FE solution could be obtained in a reasonable time

Summary

Three-dimensional modeling is necessary in the study of screw stresses and contact stresses between the bone and the plate. The FE model has demonstrated the complex nature of the structural analysis and design of internal fixation plates. The results of this study indicate the validity of the numerical modeling approach. The results also demonstrate an agreement with the mechanics of materials approach. This FE model is useful for a better understanding of the stability of implants. A typical application of the FE model will be for designing new implants that can provide better and safer fracture treatment.

Acknowledgement

This research would not have been possible without the support of the AMP program. A special thank you is extended to Professor Xiadiong Wang for sharing his knowledge of FE modeling, and Caroline Daly for her extraordinary effort in editing this paper.

Bibliography

[1] Gaffar Gailani, Ali Sadegh, Saqib Rahman. Locked and Unlocked Plating in Internal Fixation of Bones. Bio-Engineering Conference, Colorado, 2005

[2] A. Sadegh, G. Luo, and S. Cowin. Bone Ingrowth: An Application of the Boundary Element Method to Bone Remodeling at the Implant Interface. *Journal of Biomechanics*, 1993, Vol. 26, Issue 2, pp 275-284.

[3] B. R. Simon, S. L-Y Woo, G. M. Stanley, et al. Evaluation of One-, Two-, and Three-Dimensional Finite Element and Experimental Models of Internal Fixation Plates. *Journal of Biomechanics*, 1977, Vol. 10, pp.79-86.

[4] Stephan M. Perren. Evolution of the Internal Fixation of Long Bone Fractures. *British Journal of Bone Joint Surgery*, 2002, 84-B: 1093-110.

[5] J. Cordey, S. M. Perren, S.G. Steinemann. Stress Protection Due to Plates: Myth or Reality? A Parametric Analysis Made Using the Composite Beam Theory. *Injury, Int. J. Care Injured* 31, 2000, S-C1-13.

[6] Savio L-Y Woo, Bruce R. Simon, et al. A New Approach to the Design of Internal fixation Plates. *Journal of Biomedical Materials Research*, Vol. 17, 1983, 427-439.

[7] K. J. Faran, N. Ichioka, et al. Effect of Bone quality on the Forces Generated by Compression Screws. *Journal of Biomechanics*, 1992, Vol. 32, 861-864.

[8] J. Seebeck, J. Goldhahn, et al. Effect of Cortical Thickness and Cancellous Bone Density on the Holding Strength of Internal Fixator Screws. *Journal of Orthopedic Research*, 2004, Vol. 22, 1237-1242.

[9] Edward J. Cheal, Wilson C. Hayes, et al. Stress Analysis of Compression Plate Fixation and Its Effects on Long Bone Remodeling. *Journal of Biomechanics*, 1985, Vol. 18, No. 2, 141-150.

[10] VK Ganesh, K Ramakrishna and Dhanjoo N. Ghista. Biomechanics of Bone-Fracture Fixation by Stiffness-Graded Plates in Comparison with Stainless-Steel Plates. *Biomedical Engineering Online* 2005, 4:46.

- [11] ADINA R & D. ADINA Theory and Modeling Manual. Volume 1, 2001.
- [12] Pascal Swider, Annaig Pedrono, et al. Biomechanical Analysis of the Shear Behavior Adjacent to an Axially Loaded Implant. *Journal of Biomechanics*, 2005.
- [13] John D. Currey. *Bone Structure and Mechanics*. Princeton University Press, ISBN 0-691-09096-3
- [14] Klaus J. Bathe. *Finite Element Procedures*, 2nd Edition. Prentice Hall, ISBN 0-13-301458-4
- [15] S. L-Y Woo, B. R. Simon, and W. H. Akeson. An Interdisciplinary Approach to Evaluate the Effect of Internal Fixation Plate on Long Bone Remodeling. *Journal of Biomechanics*, 1977, Vol. 10, pp. 87-95.
- [16] P. Buchler, D. P. Pioletti, and L. R. Rakotomanana. Biphasic Constitutive Laws for Biological Interface Evolution. *Biomechan. Model Mechanobiology* 1, 2003, 239-249
- [17] M. Jasty, C. Bragdon, et al. In Vivo Skeletal Responses to Porous-Surfaced Implants Subjected to Small Induced Motions. *J. Bone Joint Surgery AM* 79, 1997, 707 – 714.
- [18] L. Claes. The Mechanical and Morphological Properties of Bone Beneath Internal Fixation Plates of Different Rigidity. *Journal of Orthopedic Research*, 1989, Vol. 7, pp. 170-177.

Biographies

Gaffar B. Gailani is a PhD student of Mechanical Engineering at the Graduate Center of the City University of New York. He completed his Master Degree in Mechanical Engineering in June 2001 at City College of New York. He teaches variety of courses at New York City College of Technology and Polytechnic University. His main research interests are Finite Element Modeling and CAD.

Sidi Berri Sidi Berri is an Associate Professor and the Chairman of the Mechanical Engineering and Industrial Design Technology Department of New York City College of Technology of CUNY. He completed his PhD in Mechanical Engineering at Polytechnic University. His research interests are modeling of CAD/CAM systems and Numerical Computations.

Ali Sadegh is a Professor of Mechanical Engineering at City College of New York. He received his PhD in Mechanical Engineering in Michigan State University. He is the founder and director of the Center for Advanced Engineering Design and Development. His research interests are Bone Remodeling and Implant/Bone Interaction; Computer Simulations, Design and Manufacturing. He teaches variety of courses in engineering design.